

# A novel rapid cooling assembly design in a high-pressure cubic press apparatus

Cite as: Matter Radiat. Extremes 9, 027402 (2024); doi: 10.1063/5.0176025

Submitted: 10 September 2023 • Accepted: 25 January 2024 •

Published Online: 26 February 2024




View Online



Export Citation



CrossMark

Peiyan Wu,<sup>1,2</sup>  Yongjiang Xu,<sup>1</sup>  and Yanhao Lin<sup>1,a)</sup> 

## AFFILIATIONS

<sup>1</sup> Center for High Pressure Science and Technology Advanced Research, Beijing 100193, People's Republic of China

<sup>2</sup> School of Earth Sciences and Resources, China University of Geosciences, Beijing 100083, People's Republic of China

**Note:** Paper published as part of the Special Topic on High Pressure Science 2024.

<sup>a)</sup> Author to whom correspondence should be addressed: [yanhao.lin@hpstar.ac.cn](mailto:yanhao.lin@hpstar.ac.cn)

## ABSTRACT

In traditional high-pressure–temperature assembly design, priority has been given to temperature insulation and retention at high pressures. This limits the efficiency of cooling of samples at the end of experiments, with a negative impact on many studies in high-pressure Earth and planetary science. Inefficient cooling of experiments containing molten phases at high temperature leads to the formation of quench textures, which makes it impossible to quantify key compositional parameters of the original molten phase, such as their volatile contents. Here, we present a new low-cost experimental assembly for rapid cooling in a six-anvil cubic press. This assembly not only retains high heating efficiency and thermal insulation, but also enables a very high cooling rate ( $\sim 600^\circ\text{C/s}$  from  $1900^\circ\text{C}$  to the glass transition temperature). Without using expensive materials or external modification of the press, the cooling rate in an assembly ( $\sim 600^\circ\text{C/s}$ ) with cube lengths of 38.5 mm is about ten times faster than that in the traditional assembly ( $\sim 60^\circ\text{C/s}$ ). Experiments yielding inhomogeneous quenched melt textures when the traditional assembly is used are shown to yield homogeneous silicate glass without quench textures when the rapid cooling assembly is used.

© 2024 Author(s). All article content, except where otherwise noted, is licensed under a Creative Commons Attribution (CC BY) license (<http://creativecommons.org/licenses/by/4.0/>). <https://doi.org/10.1063/5.0176025>

## I. INTRODUCTION

A cubic press is a computer-controlled anvil press with six axes [Figs. 1(a) and 1(b)], which is widely used in industry for diamond synthesis<sup>1</sup> and in high-pressure materials science and geoscience.<sup>2</sup> The six-anvil setup can generate a high pressure at the center of the sample chamber. Heating is accomplished by applying a voltage to the upper and lower anvils to create an electric current that passes through the furnace in the assembly. Temperature is measured by thermocouples located in the chamber. Compared with a multi-anvil press, one of the most widely used high-pressure–temperature devices in Earth and planetary science,<sup>3–8</sup> the assemblies used in cubic presses are easier to machine and assemble, and compression and decompression are faster (commonly several to tens of minutes for pressing to expected chamber pressure), making these presses attractive for use in industry. However, the thick pyrophyllite cube and MgO rods used in conventional cubic press assemblies (Fig. 2) hinder heat loss from the center of the assembly after quenching, resulting in a relatively slow cooling rate.

Alteration of phases due to slow cooling at the end of high-pressure experiments is a problem in a wide range of areas of materials science and Earth and planetary science and is not limited to cubic presses. Quenching of high-temperature molten phases to a homogeneous glass without quenchable textures is particularly challenging. To avoid producing an inhomogeneous silicate glass, increasing the cooling rate from melt to glass at high temperatures is key to maintaining the original composition of the melt as closely as possible,<sup>9,10</sup> both in terms of major elements and in terms of trace and volatile components (e.g., water, fluorine, chlorine, and sulfur). Recently, Bondar *et al.*<sup>7,8</sup> developed a rapid-quench octahedral assembly for a multi-anvil press based on a combination of relatively costly low-thermal-inertia materials and an external cooling system using mixtures of water and ethylene glycol. This can help to form homogeneous silicate glasses from melt at pressure–temperature conditions up to 9.3 GPa and  $1930^\circ\text{C}$ . Unfortunately, considering the differences in the design of the presses, this assembly and external cooling system are not applicable for a cubic press.

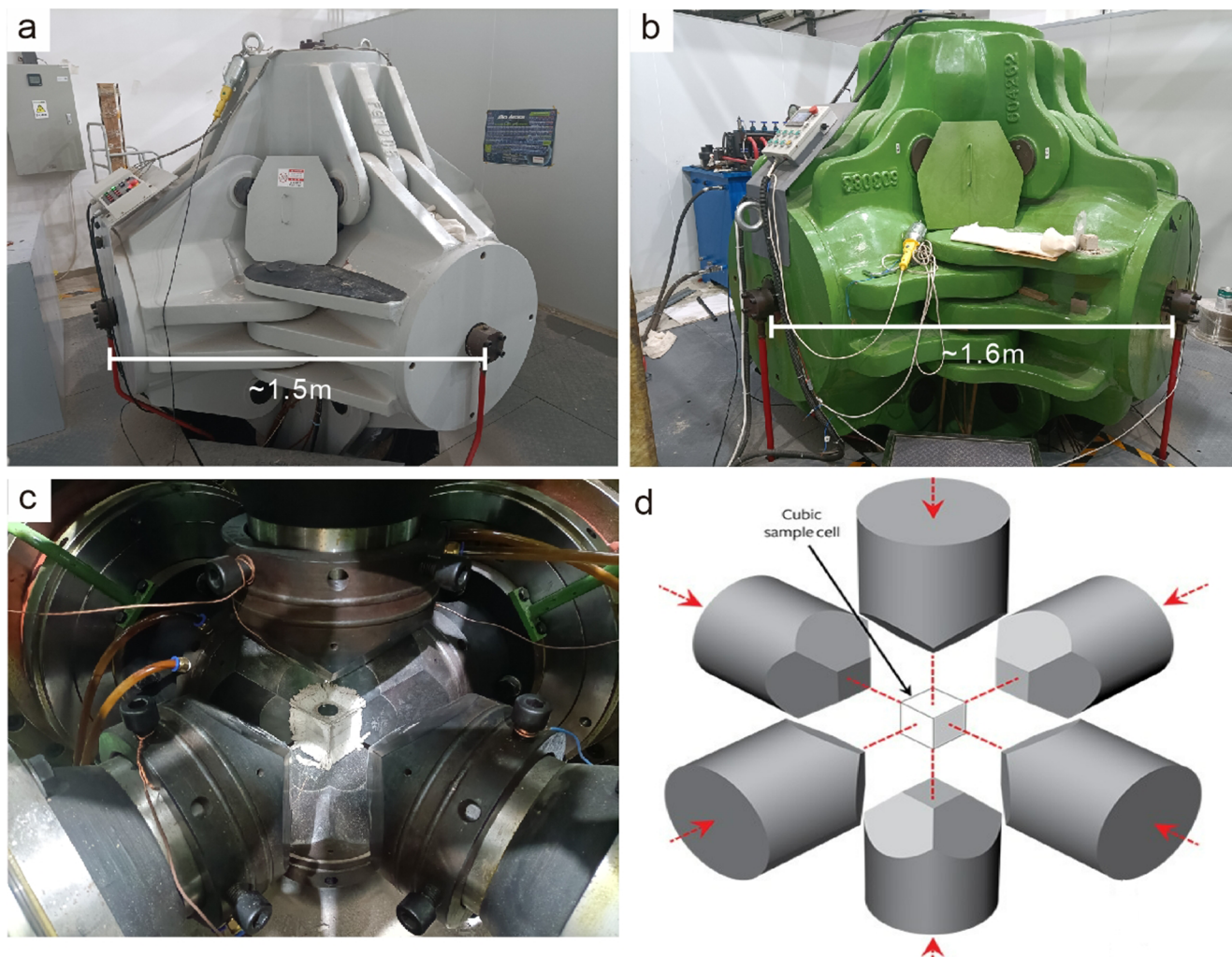


**FIG. 1.** (a) and (b) Photographs of the GY420 and GY560 cubic presses, respectively, at the HPSTAR high-pressure laboratory. (c) Photograph of six tungsten carbide (WC) anvils and a compressed cube from the GY560 cubic press. (d) Sketch of the pressurizing system of the cubic press. The six WC anvils are driven by a computer-controlled hydraulic system to generate isotropic static high pressure in the central cube from three dimensions.

In this study, we report a novel rapid-quench cubic press assembly that does not require any external modification or advanced materials, and which increases the cooling rate by a factor of about ten compared with conventional cubic press assembly designs. The effect of rapid quenching on the composition of a high-pressure silicate melt is illustrated by a comparison of test experiments on identical materials under identical conditions run with the novel and conventional designs.

## II. EXPERIMENTAL TECHNIQUES AND ANALYTICAL METHODS

### A. Experimental assembly design

Two cubic presses (GY420, applying up to  $6 \times 14$  MN force, and GY560, applying up to  $6 \times 27$  MN force) are located at the

Center for High Pressure Science and Technology Advanced Research (HPSTAR) in Beijing [Figs. 1(a) and 1(b)]. Each press has six identical jacks attached to a frame, with their actions perpendicular to each other. The jacks are driven by a computer-controlled hydraulic system. A linear sensor system around the central cubic space precisely monitors the relative positions of the six anvils. The major components of the conventional assembly consist of a natural pyrophyllite (derived from Mentougou area, Beijing) cubic block (cube edge length 38.5 mm for GY420), semi-sintered magnesium oxide sleeves, and a 10 mm inner diameter graphite furnace (Fig. 2). All parts of the assembly were dried in an oven at 120 °C for 24 h to eliminate absorbed water. The pyrophyllite cubic block serves as a pressure-transmitting medium and gasket material, and also provides structural support. The pyrophyllite block is machined to have a cubic shape and is placed around the MgO sleeves. It

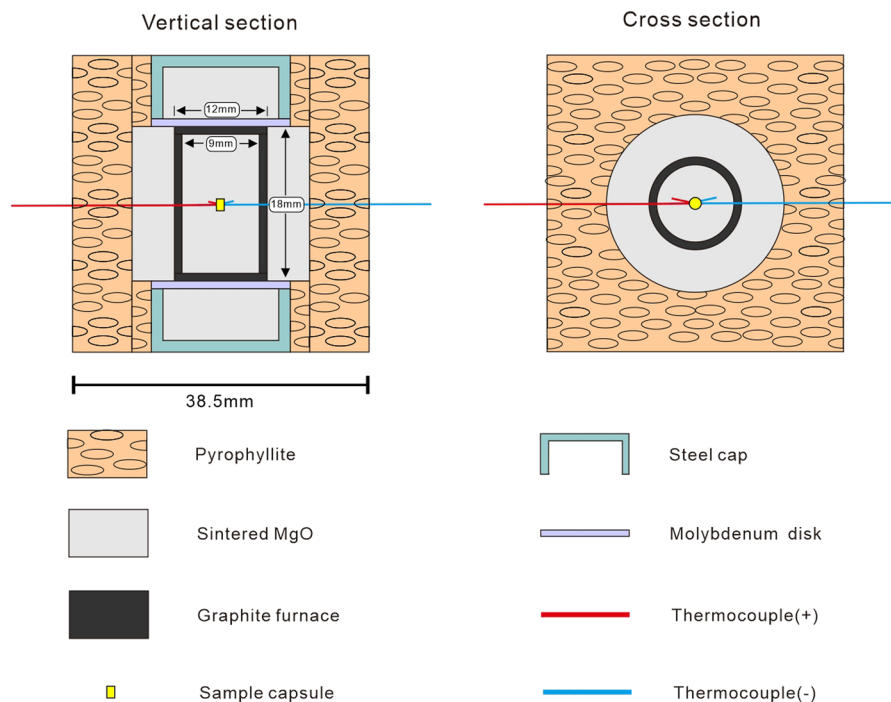


**FIG. 2.** Traditional assembly for cubic press shown in vertical and cross sections. The cube edge length is 38.5 mm.

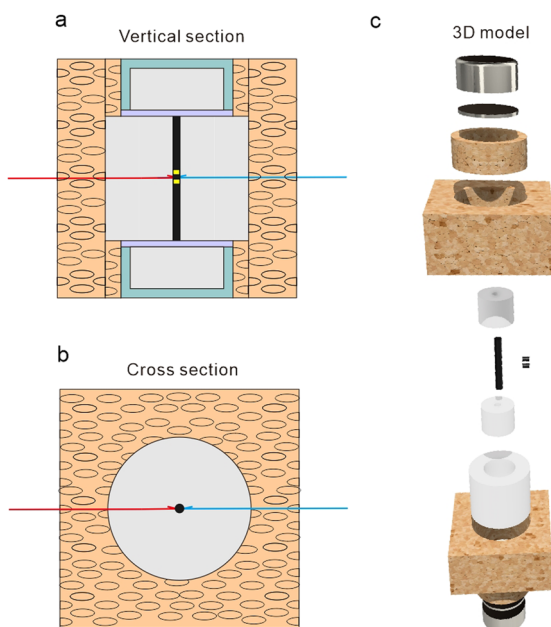


**FIG. 3.** Newly developed rapid cooling assembly shown in vertical section (a), cross section (b), and 3D model (c). For the key, see Fig. 2. A slim graphite rod (2.5 mm in diameter) is placed vertically in the center of the assembly, and sample capsules are inserted into this rod. In addition, two sample capsules can be used at the same time, symmetrically set on either side of the thermocouple junction in the center of the assembly. The cube edge length is 38.5 mm.

deforms plastically under pressure, ensuring uniform transmission of force to the center sample. The semi-sintered MgO is often used in combination with the pyrophyllite block as an additional pressure-transmitting medium to optimize pressure transmission around the tubular graphite heater with two lids. Sintered MgO rods are inserted in the tubular graphite furnace to support the sample capsule, and they also help to retain heat (Fig. 2). Temperatures are measured with radially inserted tungsten–rhenium or platinum–rhodium thermocouple wire pairs, wrapped around the sample capsule, with its junction situated in the middle of the assembly without insulator. This experimental assembly can generate pressures up to 7.6 GPa from 2.5 GPa (calibrated by the phase transition of bismuth).<sup>11</sup> The thermal properties of this assembly result in a slow cooling rate of  $>10$  s to quench a sample from 1800 to  $\sim 1000$  °C when the power is cut off. In samples containing silicate melt, this results in the formation of heterogeneous quenched crystalline glass.

To increase the experimental cooling rate, the sintered MgO rods inserted in the graphite tube heater, and the heater itself, are replaced by a thin central graphite rod of 2.5 mm diameter (Fig. 3).

## B. Starting material for test experiments

The synthetic starting material for test experiments consisted of a mixture of oxides and metals containing Si, Ti, Al, Cr, Mn, Mg, Ca, Na, K, P, Fe, S, and O. Such complex multicomponent systems are typical in high pressure-temperature studies of the initial differentiation of rocky planets, including Earth, into a metallic core

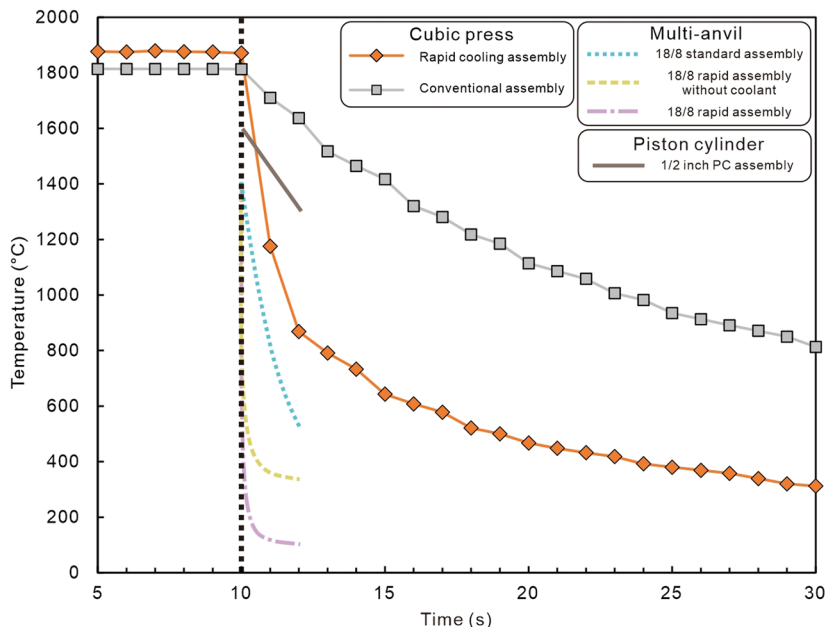


**FIG. 4.** Comparison of cooling paths between the rapid cooling assembly and the conventional assembly, after experiments at a pressure of 5 GPa and temperatures of 1800–1900 °C. The starting time of the cooling is placed at the time of the last high-temperature reading, and so the corresponding quench rates are minimum values. Previously reported cooling rate profiles<sup>7</sup> of a piston cylinder (PC) and a multi-anvil assembly are also shown.

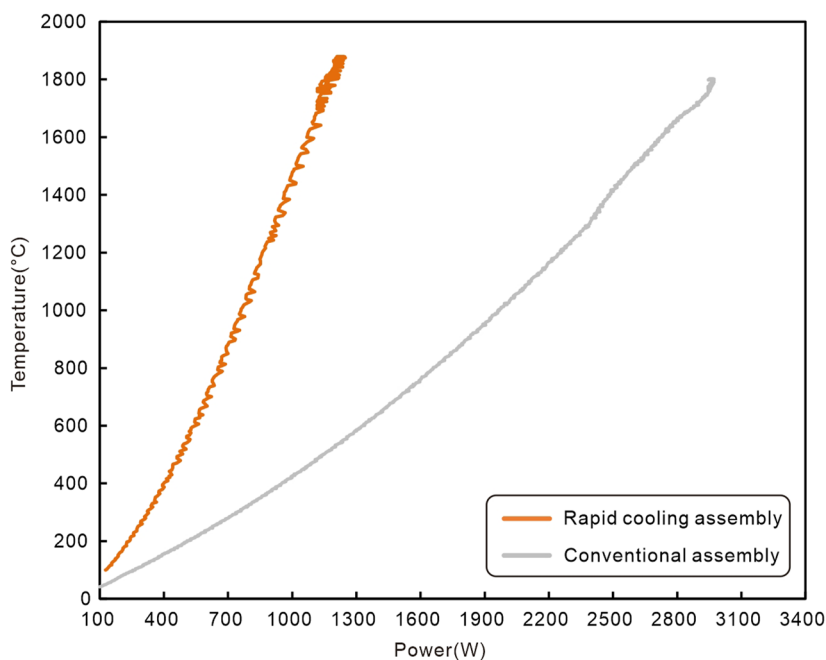


**FIG. 5.** Relation between power and temperature for the conventional and rapid cooling assemblies, demonstrating the higher nominal heating efficiency of the rapid cooling assembly.

and silicate shell. The starting material was prepared as a combination of high-purity powders:  $\text{SiO}_2$ , Si metal,  $\text{TiO}_2$ ,  $\text{Al}_2\text{O}_3$ ,  $\text{Cr}_2\text{O}_3$ , MnO, MgO,  $\text{CaSiO}_3$ ,  $\text{Na}_2\text{SiO}_3$ ,  $\text{K}_2\text{Si}_4\text{O}_9$ ,  $\text{AlPO}_4$  and FeS. These powders were mechanically mixed in appropriate proportions in an agate mortar under ethanol, dried, and then kept in a desiccator to minimize water adsorption until use. The test experiments in the conventional and novel assemblies were run at pressures of 2.5–7.6 GPa and temperatures of 1500–1900 °C for a duration of 10 min to 12 h.

### C. Analytical methods: EPMA

Run products of the test experiments were embedded in epoxy and polished using 1  $\mu\text{m}$  diamond paste. Polished samples were carbon-coated for backscattered electron (BSE) imaging to assess sample texture and phase relations. Electron microprobe analysis (EPMA) was conducted to determine the chemical compositions of constituent phases using a JEOL JXA-8230 electron microprobe at the Testing Center of the Shandong Bureau of the China Metallurgical Geology Bureau. Major and minor elements of all phases were

determined using a 15 kV accelerating voltage and a spot size of 2  $\mu\text{m}$  with a probe current of 20 nA. The standards were natural minerals and synthetic oxides for silicate phases (Si and Na, jadeite; Ti, rutile; Al, garnet; Fe, fayalite; Mg, forsterite; Ca, diopside; K, sanidine; Cr, chromite; Mn, rhodonite; P, apatite; S, pyrrhotite). Cross-sectional line measurements for both samples were carried out to check for homogeneity of major and minor element distributions.

## III. RESULTS AND DISCUSSION

### A. Performance comparisons of conventional and novel assemblies

Typical cooling paths of the traditional and novel rapid cooling experimental assemblies are shown in Fig. 4 for experiments performed at a pressure of 5 GPa and temperatures of 1800–1900 °C. Temperatures were recorded once every second. Quench rates were determined by measuring the time taken for the thermocouple reading to decrease from the initial high temperature to 1000 °C, close to the glass transition temperature in silicate melts.<sup>9,10</sup> The last thermocouple reading of the initial high temperature was taken as  $t = 0$ , and

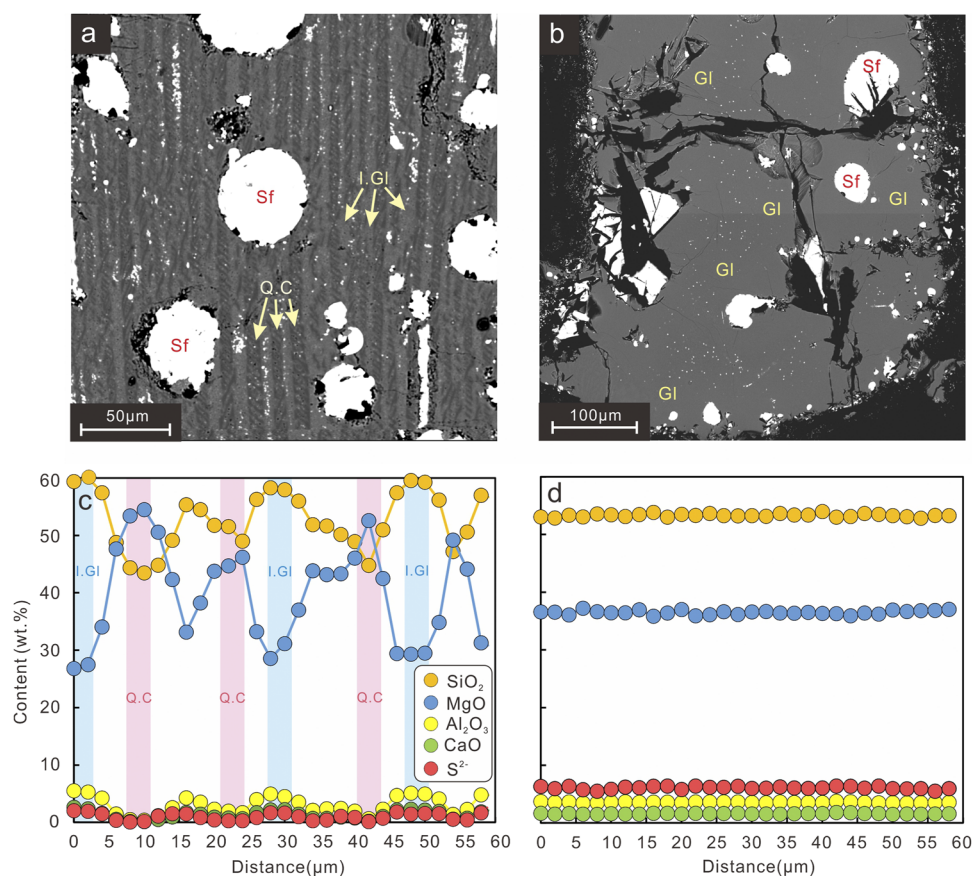


**FIG. 6.** Backscattered electron (BSE) images [(a) and (b)] and EPMA-derived chemical composition line analyses [(c) and (d)] of experiments performed at the same temperature and pressure and identical starting materials with the conventional assembly [(a) and (c)] and rapid cooling assembly [(b) and (d)]. Bright areas are S-rich iron metal; gray areas are silicate glass (light grey) and quenched minerals with interstitial silicate glass [dark grey in (a)]. Sf, iron sulfide; Q.C, quenched crystal; I.GI, interstitial silicate glass; GI, glass.

so the resulting cooling rates are minimum values. It takes about 14 s to cool down from 1800 to 1000 °C using the conventional experimental assembly (Fig. 4), whereas the rapid cooling assembly only takes a maximum of ~1.5 s to drop from a higher temperature of 1900–1000 °C (Fig. 4), equivalent to about ten times faster cooling. The cooling rate of the novel assembly is significantly slower than 6700–8200 °C/s achieved in the recently developed rapid-quench multi-anvil technique,<sup>7,8</sup> but the direct comparison cannot be made, because the structures of the assemblies used for the two devices are drastically different. One of the differences is that the volume of the assembly used in the cubic press is about 21 times larger than the 18/8 assembly used in the multi-anvil press. In practice, the cooling rate following closely the power cutoff (within several milliseconds) should be extremely high, but, nevertheless, the low recording rate of the temperature data (1 value/s) leads to the observed cooling rates being greatly underestimated. In addition, our cubic press assembly is much less expensive, is easier to manufacture and prepare, and has shorter compression and decompression times.

The nominal heating efficiency refers to the power consumption required to heat a sample to a certain temperature condition. In practice, the measured temperature depends on the physical positions of the heater and thermocouple junction (typically located at the center of the assembly). This nominal heating efficiency is significantly higher in the novel assembly, owing to the changes in the heater placement, shape, and size. With a conventional assembly, heating samples to temperatures around 1800 °C requires a power of ~3 kW. At this central assembly temperature, the WC anvils of the cubic press can reach temperatures exceeding 100 °C, close to

the upper temperature limit for safe operation of the anvils. By contrast, the power required to reach a temperature of ~1800 °C with the novel rapid-cooling assembly is only ~1 kW (Fig. 5), because the redesigned graphite rod is treated as a self-heating sample capsule, or an extra heater that improve the nominal heating efficiency. Owing to the much smaller dimensions of the furnace, under these conditions, the measured temperatures of the WC anvil in the cubic press are limited to around 50 °C, much lower than those using the conventional assembly (100–120 °C). Because the temperature distribution is more centralized with less dissipation outward, potential risks of anvil overheating can thus be significantly reduced by using the rapid cooling assembly. The comparably low temperature of the anvils also helps the cooling rate. Finally, a series of test runs have shown that the novel rapid cooling assembly can be run successfully at very high temperatures for longer durations, and with lower temperature fluctuations than the conventional assembly.

B. Test experiment run products

Figure 6 shows the results of two test experiments, run on the same starting materials under the same conditions, with the conventional and novel assemblies. The backscattered electron images of the run products show significant differences in sample textures. Although the phases of the two experiments are the same (containing S-rich iron metal and a silicate melt phase), the silicate melt phase in the experiment with the traditional assembly shows quenched skeletal olivine crystals (which grew from the melt during

TABLE I. Electron microprobe analyses of the chemical compositions of multicomponent silicate glass with and without quenchable texture taken along a profile line through the section and polished run products.

Distance (µm)	Silicate glass with quench texture														Silicate glass without quench texture													
	SiO <sub>2</sub>	TiO <sub>2</sub>	Al <sub>2</sub> O <sub>3</sub>	FeO	MgO	CaO	Na <sub>2</sub> O	K <sub>2</sub> O	Cr <sub>2</sub> O <sub>3</sub>	MnO	P <sub>2</sub> O <sub>5</sub>	S <sup>(2-)</sup>	Total	Comment <sup>a</sup>	SiO <sub>2</sub>	TiO <sub>2</sub>	Al <sub>2</sub> O <sub>3</sub>	FeO	MgO	CaO	Na <sub>2</sub> O	K <sub>2</sub> O	Cr <sub>2</sub> O <sub>3</sub>	MnO	P <sub>2</sub> O <sub>5</sub>	S <sup>(2-)</sup>	Total	
0	59.39	0.11	5.54	0.72	26.84	2.68	1.4	0.22	0.04	0.07	0.05	2.06	98.11	LGI	53.07	0.11	3.72	0.52	36.6	1.7	0.69	0.14	0.07	0.16	0	6.35	99.96	
2	60.02	0.06	5.32	0.64	27.51	2.39	0.92	0.28	0.02	0.13	0.08	1.97	98.36		52.88	0.07	3.58	0.49	36.54	1.54	0.7	0.11	0.04	0.15	0.02	5.98	99.11	
4	57.47	0.07	4.28	0.57	34.07	1.64	0.66	0.21	0.04	0.09	0.02	1.53	99.88		53.35	0.08	3.68	0.51	36.08	1.64	0.72	0.15	0.07	0.13	0	6.39	99.6	
6	48.78	0.07	1.5	0.55	47.69	0.57	0.25	0.02	0.01	0.07	0.05	0.39	99.75		53.08	0.09	3.49	0.47	37.22	1.54	0.54	0.08	0.07	0.17	0	5.8	99.63	
8	44.39	0.06	0.53	0.54	53.41	0.22	0.05	0.02	0.02	0.05	0.07	0.1	99.4		53.6	0.08	3.53	0.49	36.62	1.52	0.61	0.11	0.07	0.15	0	5.51	99.53	
10	43.5	0.02	0.42	0.6	54.51	0.18	0.05	0.01	0.04	0.05	0.03	0.2	99.49	Q.C.	53.43	0.12	3.65	0.56	36.43	1.61	0.67	0.09	0.02	0.17	0.01	5.86	99.69	
12	44.85	0.09	1.23	1.22	50.6	0.53	0.21	0.02	0.11	0.14	0.04	1.13	99.59		53.14	0.13	3.71	0.51	36.46	1.54	0.67	0.12	0.08	0.15	0	6.22	99.61	
14	49.16	0.25	2.6	2.17	42.32	1.01	0.58	0.11	0.08	0.13	0.05	1.55	99.23		53.48	0.06	3.58	0.53	36.99	1.54	0.57	0.12	0.06	0.17	0.01	6.13	100.18	
16	55.36	0.15	4.33	0.8	33.18	1.77	0.73	0.24	0.05	0.08	0.05	1.52	97.49		53.83	0.08	3.64	0.45	35.87	1.67	0.61	0.13	0.07	0.13	0.01	6.4	99.68	
18	54.52	0.08	3.56	0.47	38.26	1.48	0.57	0.08	0.04	0.11	0.08	0.89	99.7		53.03	0.08	3.61	0.53	36.39	1.68	0.76	0.15	0.03	0.12	0	6.43	99.59	
20	51.78	0.02	2.34	0.49	43.8	0.96	0.35	0.03	0.04	0.08	0.05	0.47	100.16		53.52	0.02	3.55	0.48	37.01	1.57	0.59	0.12	0.05	0.16	0	5.83	99.99	
22	51.54	0.04	1.99	0.51	44.72	0.8	0.25	0.05	0.05	0.04	0.05	0.32	100.2		53.33	0.05	3.67	0.53	35.92	1.71	0.76	0.11	0.09	0.14	0	6.44	99.52	
24	49.03	0.07	1.75	0.51	46.2	0.69	0.23	0.03	0.03	0.09	0.03	0.31	98.81		53.67	0.06	3.66	0.5	36.11	1.62	0.74	0.09	0.05	0.11	0	6.19	99.7	
26	56.3	0.05	4.01	0.46	33.25	1.75	0.7	0.16	0.05	0.07	0.06	0.86	97.29		53.29	0.02	3.65	0.51	36.63	1.65	0.69	0.11	0.04	0.14	0	6.21	99.83	
28	58.31	0.12	4.98	0.52	28.58	2.22	0.87	0.24	0	0.12	0.11	1.69	96.89	LGI	53.25	0.03	3.65	0.51	36.16	1.68	0.76	0.13	0.04	0.18	0	6.39	99.59	
30	57.97	0.1	4.54	0.55	31.17	2.26	0.8	0.23	0.02	0.1	0.07	1.66	98.63		53.3	0.09	3.55	0.54	36.59	1.58	0.7	0.1	0.05	0.15	0	6.03	99.66	
32	55.99	0.13	3.55	0.56	37.04	1.46	0.61	0.07	0.04	0.07	0.05	1.01	100.07		53.18	0.09	3.51	0.51	36.66	1.56	0.64	0.12	0.05	0.13	0.03	6.03	99.49	
34	51.91	0.05	2.14	0.5	43.85	0.73	0.24	0.05	0.03	0.05	0.03	0.33	99.72		53.68	0.06	3.65	0.49	36.42	1.55	0.71	0.09	0.08	0.14	0	6.28	100.01	
36	51.66	0.09	2.4	0.58	43.21	0.72	0.23	0.01	0.04	0.09	0.03	0.44	99.28		53.39	0.06	3.55	0.53	36.39	1.62	0.7	0.12	0.06	0.11	0	6.08	99.56	
38	50.16	0.1	2.49	1.09	43.35	0.95	0.3	0.07	0.06	0.13	0.03	1.12	99.28		53.4	0.05	3.6	0.55	36.53	1.65	0.67	0.14	0.08	0.12	0	6.01	99.81	
40	48.94	0.11	1.99	0.89	46.05	0.8	0.29	0.03	0.06	0.15	0.05	0.9	99.8		53.99	0.06	3.57	0.58	36.33	1.67	0.71	0.13	0.06	0.14	0	6.1	100.27	
42	44.8	0.02	0.68	0.54	52.6	0.24	0.07	0	0.04	0.08	0.02	0.16	99.17	Q.C.	53.04	0.09	3.77	0.45	36.29	1.83	0.74	0.13	0.08	0.12	0	6.43	99.75	
44	51	0.14	2.33	0.6	42.5	1.05	0.38	0.06	0.07	0.1	0.03	0.76	98.63		53.14	0.04	3.72	0.51	35.93	1.79	0.74	0.12	0.1	0.15	0.03	6.37	99.45	
46	57.47	0.27	4.71	0.8	29.45	2.17	0.82	0.19	0.11	0.17	0.06	1.85	97.15		53.66	0.06	3.59	0.52	36.42	1.66	0.61	0.07	0.02	0.12	0	6.06	99.76	
48	59.59	0.12	5.13	0.51	29.35	2.33	0.9	0.19	0.01	0.11	0.05	1.49	99.02	LGI	53.5	0.04	3.53	0.5	36.22	1.66	0.68	0.14	0.05	0.15	0	6.42	99.67	
50	59.3	0.14	4.99	0.45	29.52	2.17	0.89	0.17	0.02	0.12	0.02	1.58	98.58		53.31	0.06	3.52	0.48	36.94	1.52	0.72	0.11	0.04	0.13	0	5.97	99.8	
52	56.2	0.12	4.14	0.54	34.85	1.95	0.65	0.15	0.05	0.16	0.05	1.54	99.64		53.09	0.02	3.49	0.53	36.66	1.59	0.65	0.11	0.09	0.14	0	5.93	99.32	
54	47.22	0.09	1.43	0.54	49.22	0.63	0.24	0.01	0.05	0.09	0.06	0.56	99.86		52.85	0.05	3.5	0.56	36.82	1.55	0.58	0.11	0.03	0.13	0.01	5.97	99.22	
56	50.64	0.07	2.28	0.48	44.15	0.76	0.39	0.08	0.01	0.04	0.06	0.48	99.2		53.33	0.03	3.56	0.58	36.86	1.57	0.62	0.07	0.02	0.12	0	5.54	99.54	
58	57.03	0.12	4.85	0.68	31.31	1.88	0.78	0.21	0.05	0.08	0.06	1.71	97.9		53.31	0.09	3.58	0.56	37.04	1.63	0.7	0.12	0.05	0.16	0.01	5.99	100.23	
Ave.	53.36	0.1	3.24	0.74	38.78	1.42	0.55	0.11	0.04	0.1	0.05	1.13	99.62		53.34	0.06	3.6	0.52	36.5	1.62	0.67	0.11	0.06	0.14	0	6.11	99.68	
S.D.	4.63	0.08	1.49	0.51	8.05	0.74	0.31	0.08	0.04	0.04	0.02	0.72			0.27	0.03	0.07	0.03	0.35	0.08	0.06	0.02	0.02	0.02	0.01	0.25		

<sup>a</sup>LGI, interstitial glass; Q.C., quenched crystal.

the relatively long cooling time of the experiments) and interstitial glass, together with areas of clear glass, which is similar to the observations in Bondar *et al.*<sup>12</sup> By contrast, the silicate melt phase in the experiment with the novel rapid cooling assembly quenched to a single clear glass phase without quench mineral grains.

Chemical compositions of the silicate melt in both experiments, obtained through 30 spot profile analyses with the electron microprobe, are shown in Table I, with chemical point-to-point variability for several components illustrated graphically in Fig. 6. The analyses of the melt phase with the novel assembly show that the glass is very homogeneous, with very small standard deviations of the average composition of all measured components. By contrast, chemical variability is much larger in the experiment run in the conventional, slow-cooling assembly, owing to the heterogeneous distribution of quench minerals and interstitial glass. Table I also shows a significant difference between the two experiments in the abundances of the volatile element sulfur, interstitial glass, and glass. The concentration of sulfur of 6.11 ( $\pm 0.25$ ) wt. % in the free-quench-texture glass is significantly higher than the measured sulfur of 1.13 ( $\pm 0.72$ ) wt. % in the quench-crystalline glass. This suggests that significant sulfur was lost from the silicate melt phase during slow cooling and that experiments using conventional assemblies could strongly underestimate sulfur concentrations in silicate melts.

#### IV. IMPLICATIONS

The rapid cooling user-friendly assembly described in this study yields about ten times faster quenching times than conventional assemblies in a high-pressure cubic press apparatus. This enables the synthesis of texture-free glasses, which better reflect the properties of melts at high temperature. In this way, the assembly can significantly improve our understanding of the properties of silicate melts relevant to Earth and planetary science, for example, capacities of water, CO<sub>2</sub>, or S in silicate melts, and, by extension, other melts that are difficult to quench to a homogeneous glass. The test experiments illustrate that the novel rapid quench technique is particularly relevant to the geosciences, since it can enable quantification of the effects of volatiles (e.g., H<sub>2</sub>O and S) on the properties of magma and the partitioning of elements between solid mineral and silicate melt.

#### ACKNOWLEDGMENTS

We thank Wim van Westrenen and Bernard Charlier for constructive discussions and four anonymous reviewers for their constructive comments. This research was supported by National Natural Science Foundation of China Grant No. 42250105 to Y.L. The Center for High Pressure Science and Technology Advanced Research is supported by the National Science Foundation of China (Grant Nos. U1530402 and U1930401).

#### AUTHOR DECLARATIONS

##### Conflict of Interest

The authors have no conflicts to disclose.

##### Author Contributions

P.W. and Y.X. contributed equally to this work.

**Peiyan Wu:** Data curation (equal); Formal analysis (equal); Investigation (equal); Methodology (equal); Writing – original draft (equal); Writing – review & editing (equal). **Yongjiang Xu:** Data curation (equal); Formal analysis (equal); Investigation (equal); Methodology (equal); Writing – original draft (equal); Writing – review & editing (equal). **Yanhao Lin:** Conceptualization (lead); Funding acquisition (lead); Methodology (supporting); Project administration (lead); Supervision (lead); Writing – original draft (equal); Writing – review & editing (lead).

#### DATA AVAILABILITY

The data that support the findings of this study are available from the corresponding author upon reasonable request.

#### REFERENCES

- <sup>1</sup>J. Zhang, F. Liu, J. Wu, Y. Liu, Q. Hu *et al.*, “Experimental study on the pressure-generation efficiency and pressure-seal mechanism for large volume cubic press,” *Rev. Sci. Instrum.* **89**, 075106 (2018).
- <sup>2</sup>X. Zhou, D. Ma, L. Wang, Y. Zhao, and S. Wang, “Large-volume cubic press produces high temperatures above 4000 Kelvin for study of the refractory materials at pressures,” *Rev. Sci. Instrum.* **91**, 015118 (2020).
- <sup>3</sup>H. T. Hall, “Some high-pressure, high-temperature apparatus design considerations: Equipment for use at 100000 atmospheres and 3000 °C,” *Rev. Sci. Instrum.* **29**, 267–275 (1958).
- <sup>4</sup>E. Ito, “Sintered diamond multi anvil apparatus and its application to mineral physics,” *J. Mineral. Petrol. Sci.* **101**, 118–121 (2006).
- <sup>5</sup>R. Liebermann, “High pressure science and technology in Japan: A 40-year history,” *Rev. High Pressure Sci. Technol.* **21**, 115–126 (2011).
- <sup>6</sup>D. Walker and J. Li, “Castable solid pressure media for multianvil devices,” *Matter Radiat. Extremes* **5**, 018402 (2020).
- <sup>7</sup>D. Bondar, H. Fei, A. C. Withers, and T. Katsura, “A rapid-quench technique for multi-anvil high-pressure-temperature experiments,” *Rev. Sci. Instrum.* **91**, 065105 (2020).
- <sup>8</sup>D. Bondar, H. Fei, A. C. Withers, T. Ishii, A. Chanyshev, and T. Katsura, “A simplified rapid-quench multi-anvil technique,” *Rev. Sci. Instrum.* **92**, 113902 (2021).
- <sup>9</sup>S. Brawer, “Theory of relaxation in viscous liquids and glasses,” *J. Chem. Phys.* **81**, 954–975 (1984).
- <sup>10</sup>B. O. Mysen, *Silicate Glasses and Melts: Properties and Structure* (Elsevier, 2005).
- <sup>11</sup>S. Ono, “High-pressure phase transition of bismuth,” *High Pressure Res.* **38**, 414–421 (2018).
- <sup>12</sup>D. Bondar, A. Zandonà, A. C. Withers, H. Fei, D. D. Genova *et al.*, “Rapid-quenching of high-pressure depolymerized hydrous silicate (peridotitic) glasses,” *J. Non-Cryst. Solids* **578**, 121347 (2022).